

# “Uni et Trini”: In Situ Diversification of (Pyridylamide)hafnium(IV) Catalysts

Vincenzo Busico,<sup>†</sup> Roberta Cipullo,<sup>†</sup> Roberta Pellecchia,<sup>†</sup> Luca Rongo,<sup>†</sup> Giovanni Talarico,<sup>†</sup> Alceo Macchioni,<sup>‡</sup> Cristiano Zuccaccia,<sup>‡</sup> Robert D. J. Froese,<sup>§</sup> and Phillip D. Hustad<sup>\*,†,⊥</sup>

<sup>†</sup>Department of Chemistry, University of Napoli, Via Cintia, 80126, Napoli, Italy, <sup>‡</sup>Department of Chemistry, University of Perugia, Via Elce di Sotto, 8–06123, Perugia, Italy, <sup>§</sup>The Dow Chemical Company, Building 1776, Midland, Michigan 48674, and <sup>⊥</sup>The Dow Chemical Company, 2301 North Brazosport Boulevard, B-1814, Freeport, Texas 77541

Received April 9, 2009

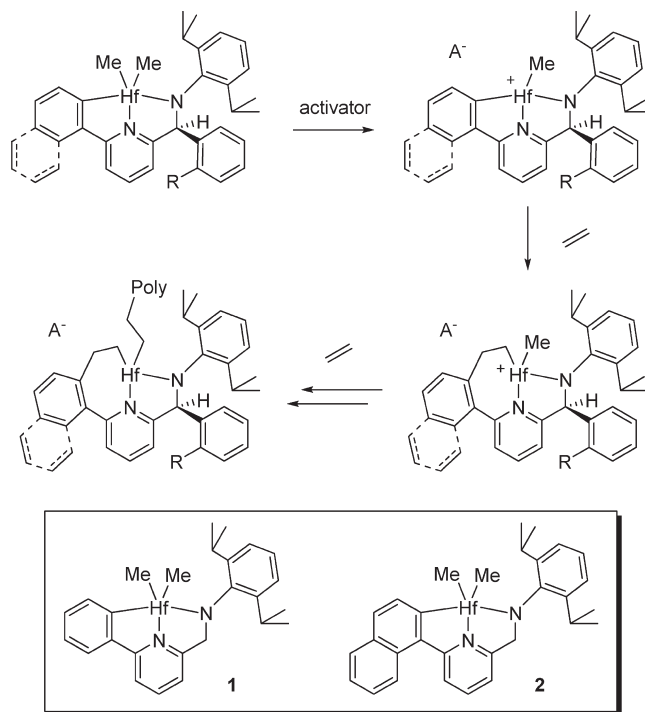
Revised Manuscript Received June 8, 2009

The recently introduced olefin polymerization catalysts derived from the (pyridylamide)Hf(IV) complexes, shown in Scheme 1,<sup>1,2</sup> are unique in many respects. From an application standpoint, they are especially remarkable for the unprecedented ability to produce high molecular weight, highly isotactic propylene homo- and copolymers in solution at high temperatures (>120 °C)<sup>3</sup> as well as olefin block copolymers with superior elastomeric properties under “chain shuttling” and coordinative chain transfer conditions.<sup>4,5</sup> In terms of scientific significance, with their nonconventional structure and the elusive nature of the active species, they represent a paradigmatic example of high throughput experimentation (HTE) based discovery.<sup>2,6,7</sup>

Two unusual features of the pyridylamide ligand framework are shown in Scheme 1. The first is the stereogenic carbon bridging the amide and the pyridine fragment, which lowers the symmetry to  $C_1$ . The second is the *ortho*-metalation of the aryl substituent bound to the pyridine, which brings the number of Hf–C  $\sigma$ -bonds amenable to olefin insertion in the active monomethyl cation to two (rather than one as is the case with most olefin polymerization catalysts). An increasing amount of experimental and computational evidence points to the fact that the Hf–C<sub>aryl</sub> bond is the most reactive site, and the true active species result from a first monomer insertion into this bond, thus modifying the precatalyst in situ (Scheme 1).<sup>8–10</sup> This hypothesis is supported by the presence of monomer-appended ligand in the catalyst residues recovered from polymerization products<sup>8</sup> and the identification of complexes with  $\sigma$ -aryl-inserted olefins.<sup>9</sup> Moreover, site-controlled isotactic polypropylene can be obtained by polymerizing propylene in the presence of catalysts derived from achiral  $C_s$ -symmetric precursors lacking the aforementioned stereogenic carbon (such as **1**<sup>10</sup> and **2** in Scheme 1), which is compelling, albeit indirect, evidence in favor of the proposed mechanism.

It should be noted at this point that Scheme 1 implies that different catalysts can be obtained from one single precatalyst. This is particularly obvious in copolymerization reactions, and indeed copolymers with broad composition and molecular weight distributions have been produced with several  $C_1$ -symmetric complexes of Scheme 1.<sup>8</sup> In homopolymerizations of 1-alkenes, a similar active site diversification may occur if insertion into the Hf–C<sub>aryl</sub> bond is not fully regio- or enantioselective. To

Scheme 1



investigate this possibility, we carried out an extensive density functional theory (DFT) study for several  $C_1$ -symmetric and  $C_s$ -symmetric precatalysts. In all cases, we conclude that the formation of multiple catalytic species is indeed likely. In the absence of a preformed stereogenic carbon, the analysis is simpler as the number of possible diastereoisomeric products is lower. Therefore, in the following, we will focus on  $C_s$ -symmetric precatalysts **1** and **2**, which are reduced to  $C_1$ -symmetry upon olefin insertion into the Hf–C<sub>aryl</sub> bond.

The four possible insertion products of propylene into the Hf–C<sub>aryl</sub> bond of a model methyl cation of **1** and **2** are shown in Figure 1, along with the DFT-calculated relative energies of the transition states (TS) leading to their formation. These values indicate that a 1,2-insertion with the enantioface yielding product **1-a** (**2-a**) is favored, but the other 1,2-insertion product (**1-b**, **2-b**) and one of the two 2,1-insertion products (**1-d**, **2-d**) can also occur with non-negligible probability. The remaining 2,1-insertion product (**1-c**, **2-c**) is much higher in energy and is not likely formed.

Following these instructive DFT studies, we investigated propylene polymerizations with precatalysts **1** and **2** in search of evidence of multisite behavior. Catalyst systems **1**/[Ph<sub>3</sub>C][B(C<sub>6</sub>F<sub>5</sub>)<sub>4</sub>] and **2**/[Ph<sub>3</sub>C][B(C<sub>6</sub>F<sub>5</sub>)<sub>4</sub>] produce polypropylene samples with very broad molecular weight distributions (MWDs,  $M_w/M_n \approx 10$  for polymerizations in toluene at 40 °C). A MWD deconvolution revealed at least three Schulz–Flory components (entries 1 and 8 of Table 1, and Figure 2a); it is certainly tempting to trace them to putative active species **1-a** (**2-a**), **1-b** (**2-b**), and **1-d** (**2-d**). The DFT-calculated regio- and stereoselectivities of all these species are similar<sup>11</sup> and compatible with the <sup>13</sup>C NMR microstructure of the polymers. The polypropylenes are moderately isotactic ([*mmmm*] = 0.37–0.41, Table 1), with stereosequence distributions indicative of site control<sup>10,12</sup> and ~3 mol % of

\*Corresponding author. E-mail: pdhustad@hotmail.com.

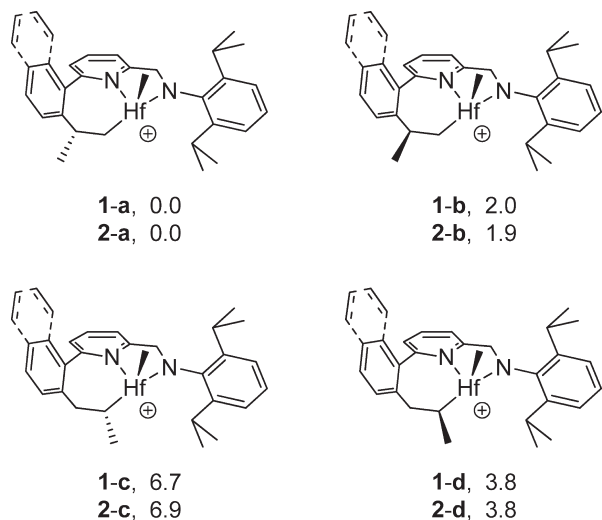


**Figure 1.** Four possible insertion products of propylene into the Hf–C<sub>aryl</sub> bond of a model methyl cation of **1** and **2** with DFT-calculated relative transition state (TS) energies (kcal mol<sup>-1</sup>, B3LYP/6-311G\*\*).

2,1-regiodefects.<sup>11</sup> Importantly, the observed microstructures are not consistent with polymerization from the simpler C<sub>3</sub>-symmetric precatalysts. The multimodal MWDs are composites of both the relative fractions of active species and their respective polymerization activities. On the basis of the calculated  $\Delta E^\ddagger$  values, species **1-b** (**2-b**) and **1-d** (**2-d**) are expected to occur at lower concentrations than **1-a** (**2-a**), but they can contribute if they have correspondingly higher activities.

An alternative and more trivial explanation for the observation of multimodal MWDs is the presence of impurities (e.g., resulting from the synthesis of the ligands) that form catalyst species with exceedingly high activities.<sup>13</sup> We carefully verified that ligands and precatalysts purified by several successive recrystallizations showed no difference in polymerization behavior. Further support against this hypothesis was obtained through polymerization of ethylene, a monomer that can yield only one *o*-aryl-inserted species with either **1** or **2**. In fact, polyethylene samples produced with catalyst systems **1**/[Ph<sub>3</sub>C][B(C<sub>6</sub>F<sub>5</sub>)<sub>4</sub>] and **2**/[Ph<sub>3</sub>C][B(C<sub>6</sub>F<sub>5</sub>)<sub>4</sub>] exhibited Schulz–Flory MWDs within the experimental uncertainty (entries 2 and 9 of Table 1).

Another difference between the two hypotheses is that, according to the mechanism in Scheme 1, the distribution of active species is expected to evolve in the early stages of the polymerization. On the basis of the relative TS energies, the probability that propylene insertion into the Hf–C<sub>aryl</sub> bond yields **1-d** (**2-d**) is fairly low (on the order of 10<sup>-3</sup>) and is comparable to that of chain transfer at the catalytic species producing the lower molecular weight polypropylene component (10<sup>-3</sup>–10<sup>-4</sup>, entries 1 and 8 of Table 1). If this mechanism is operational, polymer from species **1-d** (**2-d**) should not appear until later stages in the reaction, provided that such a phase is experimentally accessible.

With systems **1**/[Ph<sub>3</sub>C][B(C<sub>6</sub>F<sub>5</sub>)<sub>4</sub>] and **2**/[Ph<sub>3</sub>C][B(C<sub>6</sub>F<sub>5</sub>)<sub>4</sub>], the time scale of the polymerization was too fast for practical observation of short reaction times. We speculated that this problem could be overcome by using B(C<sub>6</sub>F<sub>5</sub>)<sub>3</sub> rather than [Ph<sub>3</sub>C][B(C<sub>6</sub>F<sub>5</sub>)<sub>4</sub>] as the activator, thus exploiting the known propensity of the “sticky” [Me(C<sub>6</sub>F<sub>5</sub>)<sub>3</sub>]<sup>-</sup> anion to slow the polymerization.<sup>14</sup> In fact, a “living” character at 25 °C has been recently reported for **1**/B(C<sub>6</sub>F<sub>5</sub>)<sub>3</sub>.<sup>10</sup> The results of propylene polymerization runs at 40 °C and variable reaction times (*t*<sub>p</sub>) with **1**/B(C<sub>6</sub>F<sub>5</sub>)<sub>3</sub> and **2**/B(C<sub>6</sub>F<sub>5</sub>)<sub>3</sub> are given in Table 1 (entries 3–7 and 10–14, respectively). As expected, the polymerization rates were much lower than with [Ph<sub>3</sub>C][B(C<sub>6</sub>F<sub>5</sub>)<sub>4</sub>] activation.

**Table 1.** Results of propylene and ethylene polymerizations at 40 °C and characterization data for polymers, including <sup>13</sup>C NMR, GPC and MWD deconvolution.<sup>a</sup>

catalyst system <sup>b</sup>	entry	olefin <sup>c</sup>	<i>t</i> <sub>p</sub> , min	<i>Y</i> <sub>p</sub> <sup>d</sup>	[mmmm] <sup>e</sup>	component #1			component #2			component #3		
						<i>M</i> <sub>n</sub> , MDa	<i>M</i> <sub>w</sub> / <i>M</i> <sub>n</sub>	<i>w</i> <sub>1</sub>	<i>M</i> <sub>n</sub> , MDa	<i>M</i> <sub>w</sub> / <i>M</i> <sub>n</sub>	<i>w</i> <sub>2</sub>	<i>M</i> <sub>n</sub> , MDa	<i>M</i> <sub>w</sub> / <i>M</i> <sub>n</sub>	<i>w</i> <sub>3</sub>
<b>1</b> /borate	1	C <sub>3</sub> H <sub>6</sub>	5	4.7 × 10 <sup>3</sup>	0.41	0.14	8.8	0.45(8)	0.30(5)	2.00	0.44(6)	1.7(5)	2.00	0.12(3)
	2	C <sub>2</sub> H <sub>4</sub>	10	1.3 × 10 <sup>4</sup>	0.36	0.48	2.2							
	3	C <sub>3</sub> H <sub>6</sub>	10	2.3 × 10 <sup>2</sup>	n.d. <sup>e</sup>	0.07	1.4							
<b>1</b> /borane	4		20	2.7 × 10 <sup>2</sup>	n.d.	0.10	1.4							
	5		40	3.1 × 10 <sup>2</sup>	n.d.	0.22	5.1	0.76(7)	0.51(9)	1.5	0.24(7)			
	6		120	1.4 × 10 <sup>2</sup>	n.d.	0.22	7.5	0.66(2)	0.7(3)	2.00	0.31(8)	8	2.00	0.03
	7		180	0.9 × 10 <sup>2</sup>	0.36	0.11	13.9	0.60(5)	0.5	2.00	0.36(5)	7	2.00	0.04
<b>2</b> /borate	8	C <sub>3</sub> H <sub>6</sub>	5	3.1 × 10 <sup>3</sup>	0.37	0.17	11.4	0.51(7)	0.54	2.00	0.35(8)	2.8	2.00	0.15(7)
	9	C <sub>2</sub> H <sub>4</sub>	10	8.9 × 10 <sup>2</sup>	0.53	0.08	2.3							
<b>2</b> /borane	10	C <sub>3</sub> H <sub>6</sub>	3	6.2 × 10 <sup>2</sup>	0.38	0.09	4.3	0.63(3)	0.69(5)	1.20(4)	0.37(3)			
	11		7	7.8 × 10 <sup>2</sup>	n.d.	0.096(2)	6.2	0.62(2)	1.10(7)	2.00	0.38(2)			
	12		10	5.2 × 10 <sup>2</sup>	n.d.	0.16	8.9	0.66(2)	1.4(2)	2.00	0.34(2)			
	13		20	4.4 × 10 <sup>2</sup>	n.d.	0.26	18	0.68(3)	1.0(4)	2.00	0.16(3)	6	2.00	0.17(3)
	14		30	3.6 × 10 <sup>2</sup>	0.36	0.28	31	0.76(4)	1.5(8)	2.00	0.13(3)	14	2.00	0.11(2)

<sup>a</sup> Uncertainty (standard deviation): ±1 on last significant digit if not indicated otherwise. <sup>b</sup> Borate = [Ph<sub>3</sub>C][B(C<sub>6</sub>F<sub>5</sub>)<sub>4</sub>], borane = B(C<sub>6</sub>F<sub>5</sub>)<sub>3</sub>. <sup>c</sup> Olefin: C<sub>2</sub>H<sub>4</sub> = ethylene, C<sub>3</sub>H<sub>6</sub> = propylene. <sup>d</sup> Productivity in kg × mol<sub>Hf</sub><sup>-1</sup> × h × [C<sub>3</sub>H<sub>6</sub>]<sup>-1</sup>; lower limit values, as no scavenger was used. <sup>e</sup> <sup>13</sup>C NMR fraction of isotactic pentads. <sup>f</sup> n.d. = not determined.

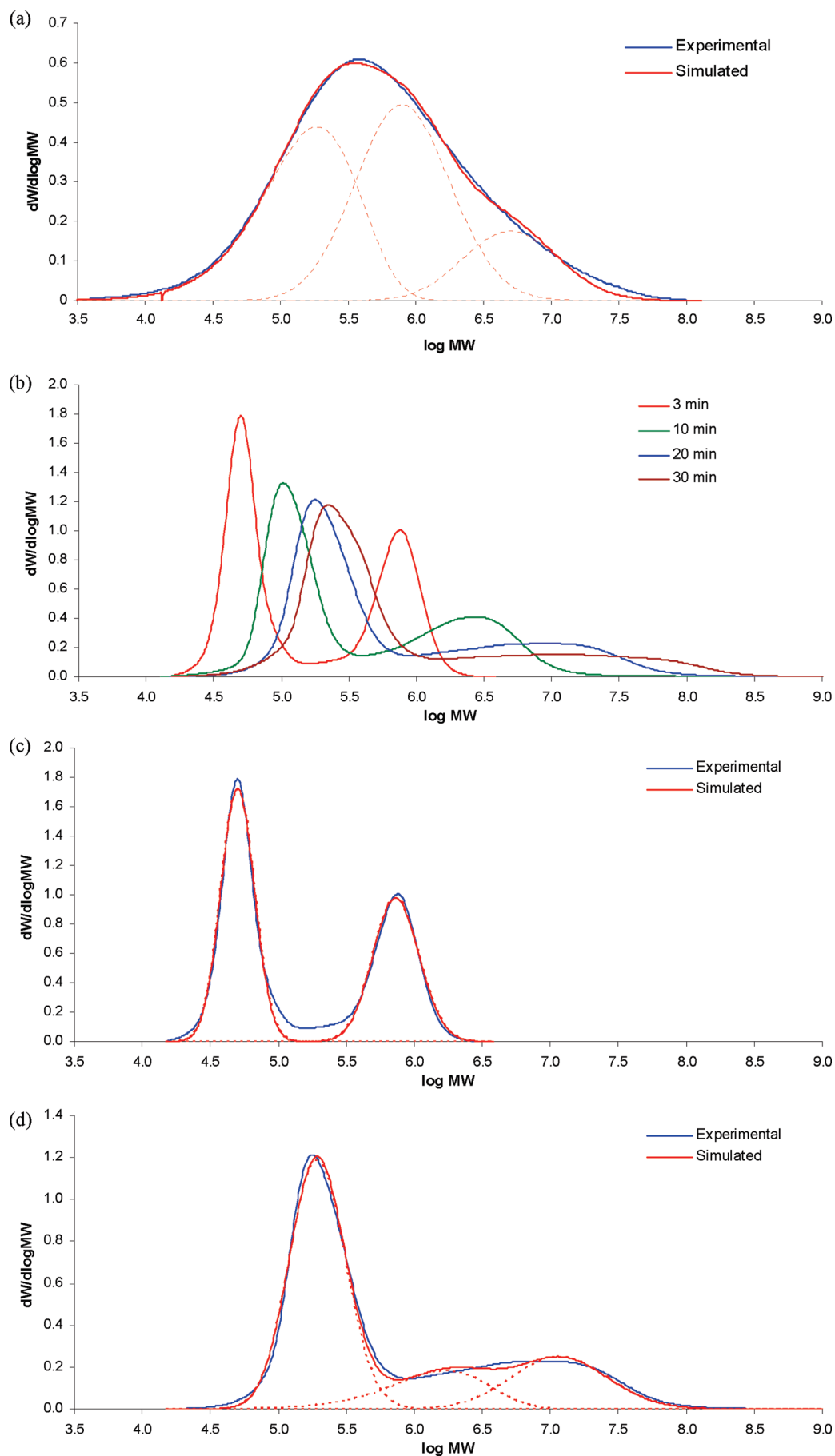


**Figure 2.** Experimental and simulated MWD of polypropylene samples obtained at 40 °C with  $2/[Ph_3C][B(C_6F_5)_4]$  and  $2/B(C_6F_5)_3$  (Table 1: (a) entry 8; (b) entries 10, 12, 13, 14; (c) entry 10; (d) entry 13).

In line with the hypothesis of in situ catalyst speciation, an interesting time evolution of the polymer MWD was observed (Figure 2b).

The polymers obtained with **2**/ $\text{B}(\text{C}_6\text{F}_5)_3$  have a bimodal MWD at short  $t_p$ , with two Poisson-like components typical of controlled chain growth (entry 10 of Table 1 and Figure 2c).<sup>15</sup> With increasing  $t_p$ , one of the two peaks changed rapidly into a Schulz–Flory function (entries 11–12 of Table 1) as it reached the plateau value of  $M_n$ . At longer reaction times, the MWD became trimodal (entries 13–14 of Table 1 and Figure 2d) due to a third component with very high molecular weight. This component appeared directly as a Schulz–Flory function, indicative of very fast nonliving polymerization kinetics for the active species producing it.

Analogous behavior was observed for **1**/ $\text{B}(\text{C}_6\text{F}_5)_3$ , although with even slower kinetics and a lower resolution of the polymer MWDs (entries 3–7 of Table 1). It is important to note that for both systems, the overall MWDs at long  $t_p$  become rather similar to those observed with  $[\text{Ph}_3\text{C}][\text{B}(\text{C}_6\text{F}_5)_4]$ -activation (compare entries 1 and 7, and 8 and 14 of Table 1). The agreement is reasonable considering the (admittedly large) error attached to the experimental and deconvoluted MWD results and the different nature of the anions. It is also worth noting that the relative TS energies from preliminary DFT calculations<sup>11</sup> reveal that the distribution of active catalysts is slightly altered with different activators, although the prominent species are expected to be the same.

In our opinion, the above factual observations are all compatible with the hypothesis of in situ speciation of catalysts **1-a** (**2-a**), **1-b** (**2-b**), and **1-d** (**2-d**) from precatalysts **1** and **2**. This, however, remains a hypothesis. While we are convinced that in situ speciation from aryl insertion generates multiple sites, the precise assignment of the active species based on DFT is not dependable. Many literature examples have demonstrated that small changes near the metal center can lead to vastly different activities and polymer characteristics,<sup>16</sup> and we can only surmise that the differences arise from the subtle combination of these steric and electronic factors. We also note that an increase in the average polymer molecular weight with increasing monomer insertion rate is to be expected when the dominant chain transfer pathway is intramolecular  $\beta$ -H elimination, which is the case in general with (pyridylamide)Hf catalysts.<sup>17</sup> As a matter of fact, comparatively low values of catalyst productivity and average polymer molecular weights were observed with ethylene (entries 2 and 9 of Table 1), which might be traced to the marked absence of species like **1-d** (**2-d**).

Other possibilities for the identity of the active sites, on the other hand, cannot be ruled out at the present stage. For instance, a second layer of complexity would arise if species **1-a** (**2-a**), **1-b** (**2-b**), and **1-d** (**2-d**) were capable of isomerization into other species. Possible pathways for isomerization include a metallocycle ring flip or  $\beta$ -H elimination of the alkylaryl moiety followed by olefin rotation and reinsertion into the Hf–H bond. A preliminary computational investigation has thus far failed to find a viable pathway, but isomerizations have been reported for similar cyclometalated species.<sup>18,19</sup>

In all cases, though, an important lesson should be learned from this story. At odds with the common belief that “single-site” olefin polymerization catalysis is easily amenable to rational understanding (a confidence grown along with metallocenes<sup>20</sup>), it is clear that molecular catalysts are not necessarily simple nor foreseeable. In our opinion, precatalysts like those of Scheme 1<sup>1,2</sup> are beyond the reach of rational design. As a matter of fact, the presence of a stereogenic carbon in the chiral precursors results in a formidable complication of catalyst speciation. Considering the higher number of diastereoisomers possible upon insertion of a 1-alkene into the Hf–C<sub>aryl</sub> bond, it is likely that the “true” catalytic

species of these systems will not be identified with certainty.<sup>8,9</sup> This demonstrates that serendipitous discovery, now aided by powerful HTE tools and methods,<sup>2,6,7</sup> remains an important option for further progress in the field.

**Acknowledgment.** The authors wish to thank Sara Ronca for precatalyst preparation, Francesca Alfano for assistance in part of the polymerization experiments, and Michele Vacatello, Roger Kuhlman, Tim Wenzel, Paul Vosejпка, and James Stevens for valuable discussions.

**Supporting Information Available:** Text giving detailed experimental procedures for the preparation and characterization of the Hf precatalysts, propylene and ethylene polymerization experiments (including a table of data), and NMR (including a table of data) and GPC polymer characterizations, and computational details including methods and tables of Cartesian coordinates and total energies and figures showing the structure of 2,6-diisopropyl-*N*-((6-phenylpyridin-2-yl)methyl)aniline, GPC traces, and transition states. This material is available free of charge via the Internet at <http://pubs.acs.org>.

## References and Notes

- (1) (a) Boussie, T. R.; Diamond, G. M.; Goh, C.; Hall, K. A.; LaPointe, A. M.; Leclerc, M. K.; Lund, C.; Murphy, V. U.S. Patent Appl. Publ. No. 0135722 A1, **2006**. (b) Boussie, T. R.; Diamond, G. M.; Goh, C.; Hall, K. A.; LaPointe, A. M.; Leclerc, M. K.; Lund, C.; Murphy, V. U.S. Pat. 7,018,949, **2006**. (c) Boussie, T. R.; Diamond, G. M.; Goh, C.; LaPointe, A. M.; Leclerc, M. K.; Lund, C.; Murphy, V. U.S. Pat. 6,750,345, **2004**. (d) Boussie, T. R.; Diamond, G. M.; Goh, C.; Hall, K. A.; LaPointe, A. M.; Leclerc, M. K.; Lund, C.; Murphy, V. U.S. Pat. 6,713,577, **2004**. (e) Boussie, T. R.; Diamond, G. M.; Goh, C.; Hall, K. A.; LaPointe, A. M.; Leclerc, M. K.; Lund, C.; Murphy, V. U.S. Pat. 6,706,829, **2004**. (f) Boussie, T. R.; Diamond, G. M.; Goh, C.; Hall, K. A.; LaPointe, A. M.; Leclerc, M. K.; Lund, C.; Murphy, V. PCT Int. Publ. No. WO 046249, **2002**. (g) Boussie, T. R.; Diamond, G. M.; Goh, C.; Hall, K. A.; LaPointe, A. M.; Leclerc, M. K.; Lund, C.; Murphy, V. PCT Pat. Publ. No. WO 038628, **2002**.
- (2) Boussie, T. R.; Diamond, G. M.; Goh, C.; Hall, K. A.; LaPointe, A. M.; Leclerc, M. K.; Murphy, V.; Shoemaker, J. A. W.; Turner, H.; Rosen, R. K.; Stevens, J. C.; Alfano, F.; Busico, V.; Cipullo, R.; Talarico, G. *Angew. Chem., Int. Ed.* **2006**, *45*, 3278.
- (3) (a) Arriola, D. J.; Bokota, M.; Timmers, F. J. PCT Int. Publ. No. WO026925 A1, **2004**. (b) Frazier, K. A.; Boone, H.; Vosejпка, P. C.; Stevens, J. C. U.S. Pat. Pub. No. 0220050 A1, **2004**. (c) Tau, L.-M.; Cheung, Y. W.; Diehl, C. F.; Hazlitt, L. G. U.S. Pat. Pub. No. 0087751 A1, **2004**. (d) Tau, L.-M.; Cheung, Y. W.; Diehl, C. F.; Hazlitt, L. G. U.S. Pat. Pub. No. 0242784 A1, **2004**. (e) Coalter, J. N., I. I. I.; Van Egmond, J. W.; Fouts, L. J., Jr.; Painter, R. B.; Vosejпка, P. C. PCT Int. Publ. No. WO 040195 A1, **2003**. (f) Stevens, J. C.; Vanderlende, D. D. PCT Int. Publ. No. WO 040201 A1, **2003**.
- (4) Arriola, D. J.; Carnahan, E. M.; Hustad, P. D.; Kuhlman, R. L.; Wenzel, T. T. *Science* **2006**, *312*, 714.
- (5) Hustad, P. D.; Kuhlman, R. L.; Arriola, D. J.; Carnahan, E. M.; Wenzel, T. T. *Macromolecules* **2007**, *40*, 7061.
- (6) Murphy, V.; Bei, X.; Boussie, T. R.; Brummer, O.; Diamond, G. M.; Goh, C.; Hall, K. A.; LaPointe, A. M.; Leclerc, M.; Longmire, J. M.; Shoemaker, J. A. W.; Turner, H.; Weinberg, W. H. *Chem. Record* **2002**, *2*, 278.
- (7) Boussie, T. R.; Diamond, G. M.; Goh, C.; Hall, K. A.; LaPointe, A. M.; Leclerc, M. K.; Lund, C.; Murphy, V.; Shoemaker, J. A. W.; Tracht, U.; Turner, H.; Zhang, J.; Uno, T.; Rosen, R. K.; Stevens, J. C. *J. Am. Chem. Soc.* **2003**, *125*, 4306.
- (8) Froese, R. D. J.; Hustad, P. D.; Kuhlman, R. L.; Wenzel, T. T. *J. Am. Chem. Soc.* **2007**, *129*, 7831.
- (9) Zuccaccia, C.; Macchioni, A.; Busico, V.; Cipullo, R.; Talarico, G.; Alfano, F.; Boone, H. W.; Frazier, K. A.; Hustad, P. D.; Stevens, J. C.; Vosejпка, P. C.; Abboud, K. A. *J. Am. Chem. Soc.* **2008**, *130*, 10354.
- (10) Domski, G. J.; Lobkovsky, E. B.; Coates, G. W. *Macromolecules* **2007**, *40*, 3510.
- (11) See Supporting Information for further details.
- (12) Busico, V.; Cipullo, R. *Prog. Polym. Sci.* **2001**, *26*, 443.

- (13) Niu, H.; Stellbrink, J.; Allgaier, J.; Richter, D.; Hartmann, R.; Domski, G. J.; Coates, G. W.; Fetters, L. J. *Macromolecules* **2009**, *42*, 1083.
- (14) Chen, E. Y.-X.; Marks, T. J. *Chem. Rev.* **2000**, *100*, 1391.
- (15) (a) Domski, G. J.; Rose, J. M.; Coates, G. W.; Bolig, A. D.; Brookhart, M. *Prog. Polym. Sci.* **2007**, *32*, 30. (b) Coates, G. W.; Hustad, P. D.; Reinartz, S. *Angew. Chem., Int. Ed.* **2002**, *41*, 2236.
- (16) For an example of the dramatic influence of indene substitution on propylene polymerization characteristics using *rac*-bisindenylzirconocenes, see: Spaleck, W.; Kueber, F.; Winter, A.; Rohrmann, J.; Bachmann, B.; Antberg, M.; Dolle, V.; Paulus, E. F. *Organometallics* **1994**, *13*, 954.
- (17) Froese, R. D. J.; Talarico, G. Unpublished results.
- (18) For an example of isomerization in a similar cyclometallated complex proposed to occur via ring flip, see: Domski, G. J.; Edson, J. B.; Keresztes, I.; Lobkovsky, E. B.; Coates, G. W. *Chem. Commun.* **2008**, *46*, 6137.
- (19) For an example of isomerization via  $\beta$ -elimination and reinsertion, see: Gielens, E. E. C. G.; Dijkstra, T. W.; Berno, P.; Meetsma, A.; Hessen, B.; Teuben, J. H. *J. Organomet. Chem.* **1999**, *591*, 88.
- (20) (a) Brintzinger, H.-H.; Fischer, D.; Muelhaupt, R.; Rieger, B.; Waymouth, R. M. *Angew. Chem., Int. Ed. Engl.* **1995**, *34*, 1143. (b) Resconi, L.; Cavallo, L.; Fait, A.; Piemontesi, F. *Chem. Rev.* **2000**, *100*, 1253.